(REVIEW ARTICLE)

Investigation of electrical properties of CH₃NH₃Sn(I₁₋ₓClₓ)₃ perovskite solar cell by SCAPS-1D simulation

Rejowan Ahmed Biplob *

Department of Electrical and Electronic Engineering, Gono Bishwabidyalay, Dhaka, Bangladesh.

Abstract

In this research, we developed a tin-based eco-friendly $CH_3NH_3Sn(I_{1-x}Cl_x)_3$ perovskite solar cell to simulate the architecture $FTO/TiO_2/CH_3NH_3Sn(I_{1-x}Cl_x)_3/Cu_2O$ by using the SCAPS-1D. We have studied the effect of the performance of solar cells by varying thickness, band gap energy, doping acceptor density, and total defect density of absorber layer-$CH_3NH_3Sn(I_{1-x}Cl_x)_3$ through the software tool. At first, we simulate the device and find the performance of electrical properties such as efficiency, based on the parameters that are taken from the previous research paper. Later we vary only on the absorber layer parameters mentioned above, to get the optimum results of the designed solar cell. The efficiency for the plugging parameters value and after applying the parameter obtained optimum value jumped from 27.83% to 39.28%. After optimizing all the properties, the efficiency has been enhanced by about 11.45%.

Keywords: Perovskite Solar cell; SCAPS-1D; Power conversion efficiency (PCE); Defect density; Renewable energy

1. Introduction

These days, the prerequisite for renewable energy has developed quickly over the last decade due to industrialization and increasing populations. Nonrenewable energy reserves will be depleted in the coming days. Solar energy devices will be an unobjectionable solution in a global energy crisis [2-3]. In the photovoltaic effect, sunlight directly converts into electricity. This process involves the absorption of photons by semiconductor material within the solar cell, which generates electron-hole pairs and thus creates a voltage potential. Key electrical properties of solar cells include efficiency, voltage, current, and fill factor, which collectively determine the cell's overall performance and stability for various applications. The SCAPS-1d software simulation tools have been used to simulate $CH_3NH_3Sn(I_{1-x}Cl_x)_3$ Perovskite Solar Cells (PSCs) electrical properties study on performance. PSCs, or perovskite solar cells, have gained massive attention in recent years due to their touted high efficiency, low-cost fabrication, and versatility. These solar cells are constructed using materials featuring a perovskite crystal structure, typically comprising organic-inorganic hybrid compounds. At the heart of the PSC lies the perovskite absorber layer, responsible for absorbing sunlight and generating charge carriers. Traditionally, lead-based perovskite materials have been utilized for high performance. However, research is ongoing to explore lead-free alternatives due to concerns regarding lead toxicity and stability. We know that double-halide gives us more thermal stability than single-halide so in this work we used $(I_{1-x}Cl_x)_3$ double-halide material for long-term stability [1]. PSCs performance has increased tremendously recently. It has shown that photovoltaic power conversion efficiency has jumped from 3.8% in 2009 [3] to 29.8% in 2023 [4-5]. Lead-based perovskite materials showed a high power conversion efficiency value but are not eco-friendly, which is harmful to humans and the environment [6].

---

* Corresponding author: Rejowan Ahmed Biplob

2. Material and simulation model

In this study, a numerical simulation of a planar heterojunction tin-based $CH_3NH_3Sn(I_{1-x}Cl_x)_3$ PSCs has been performed using SCAPS. We have discussed the structure comprising $FTO/TiO_2/CH_3NH_3Sn(I_{1-x}Cl_x)_3 /Cu_2O$ is shown in Figure 1. In which fluorine-doped tin oxide (FTO) is used as a front contact material, TiO_2 as electron transport material (ETM), $CH_3NH_3Sn(I_{1-x}Cl_x)_3$ as an absorber layer, and copper-based materials Cu_2O as hole transport layer (HTL) [7-12].
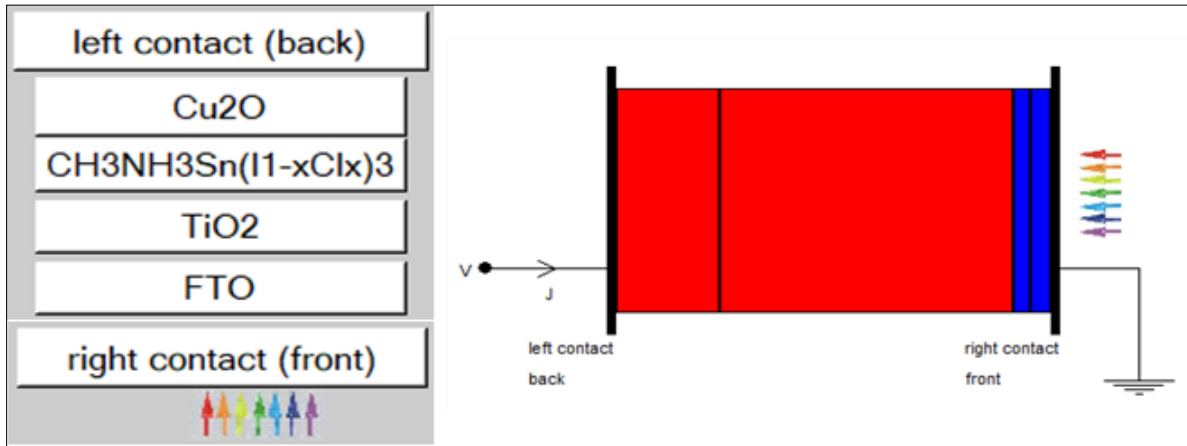
Figure 1 Structural architecture of $FTO/TiO_2/CH_3NH_3Sn(I_{1-x}Cl_x)_3 /Cu_2O$

To show the performance parameters of the device like current density–voltage (J-V) curve, quantum efficiency, Open circuit voltage, and short circuit current according to change thickness, bandgap, acceptor density, and total defect density of the absorber layer at temperature 300K.

Table 1 SCAPS Simulation parameters value for each layer

Parameter	Cu_2O	$CH_3NH_3Sn(I_{1-x}Cl_x)3$	TiO_2	FTO
Thickness (μm)	0.25	0.700	0.04	0.05
Band Gap (eV)	2.17	1.30	3.2	3.50
Electron Affinity (eV)	3.2	4.17	3.9	4.0
Dielectric Permittivity (relative)	7.11	6.5	9.0	9.0
Conduction band effective density of states (cm^{-3})	2.02×10^{17}	1×10^{18}	1×10^{21}	2.20×10^{18}
Valance band effective density of states (cm^{-3})	1.1×10^{19}	1×10^{19}	1×10^{20}	1.8×10^{18}
Electron thermal velocity (cm/s)	1×10^7	1×10^7	1×10^7	1×10^7
Hole thermal velocity (cm/s)	1×10^7	1×10^7	1×10^7	1×10^7
Electron Mobility (cm^2/Vs)	2×10^2	1.6	20	20
Hole Mobility (cm^2/Vs)	8×10^1	1.6	1×10^1	1×10^1
Shallow uniform donor density ND (1/cm3)	0	0	1×10^{19}	1×10^{19}
Shallow uniform acceptor density NA (1/cm3)	1×10^{18}	3.2×10^{15}	1	0
Total Defect density, Nt (1/cm3)	1×10^{14}	1×10^{14}	1×10^{14}	1×10^{15}

Designed device material Thickness (μm), Band Gap (eV), Electron Affinity (eV), Dielectric Permittivity (relative), Conduction band effective density of states (cm^{-3}), Valence band effective density of states (cm^{-3}), Electron thermal velocity (cm/s), Hole thermal velocity (cm/s), Electron Mobility (cm^2/Vs), Hole Mobility (cm^2/Vs), Shallow uniform donor density ND (1/cm3), Shallow uniform acceptor density NA (1/cm3), Total Defect density Nt (1/cm3) values are taken from theories, experiments and literature are shown in Tables 1 [5-6] [13-16].

3. Results and discussion

3.1. Current- Voltage analysis

The designed structure of PSCs, electrical characteristic voltage vs current density is represented in Figure 2, based on the parameters from Table 1. The resulting J-V curve is obtained under the temperature at 300K. The device has shown open circuit voltage (V_{oc}) of 0.9801V, short circuit current density (Jsc) of 33.999 mA/cm^2, fill factor (FF) of 83.51%, and power conversion efficiency (PCE) of 27.83%.
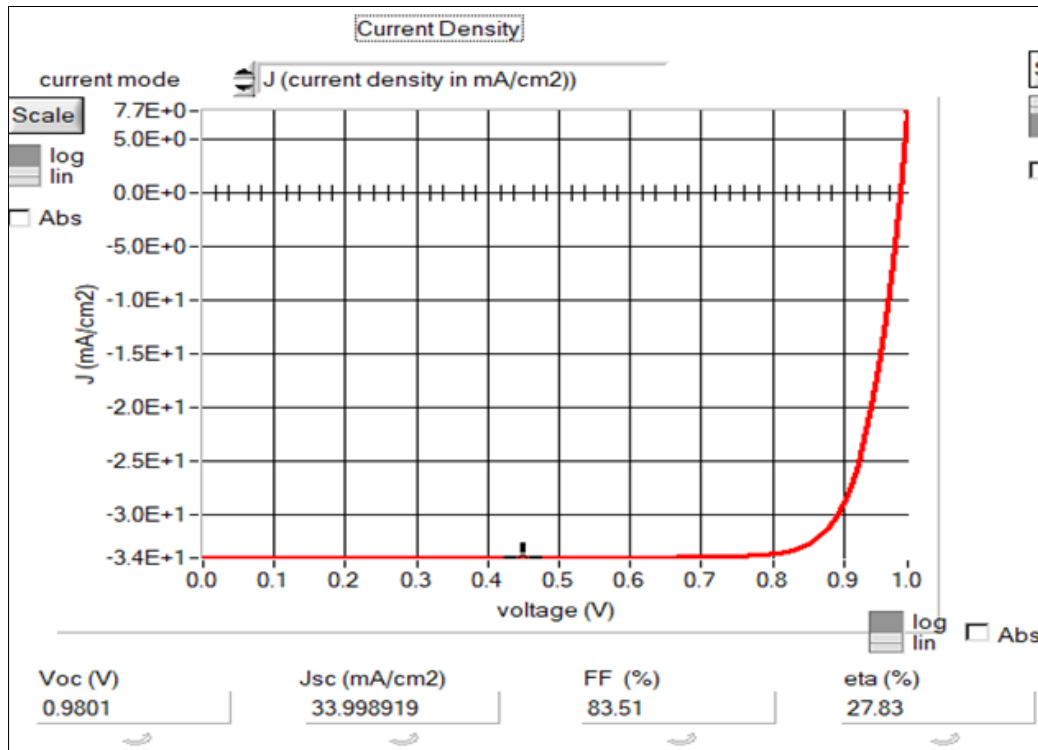
Figure 2 J-V curve of the structured solar cell using SCAPS-1D

In these sections, by considering the final results, the effect of some essential layer parameters on the device performance has been studied. In addition to the photovoltaic parameters of the studied cell, we considered the results for selecting the appropriate parameter for the absorber layer.

3.2. Effect of absorber layer thickness

The $CH_3NH_3Sn(I_{1-x}Cl_x)_3$ absorber layers play a massive role in electrical performance due to the change of thickness. The thickness value has changed from 0.3 μm to 1.5 μm. The performance parameters such as efficiency (eta), FF, Voc, Jsc, V_mpp, and I_mpp of the solar cells with varying thicknesses are shown in Figure 3. The thickness is varied from 0.3 μm to 1.5μm to find the optimal value of thickness for best performance. From the thickness vs efficiency curve, due to increases in the absorber layer thickness, the efficiency increases. The curve gives a maximum efficiency of 28.08%, fill factor of 83.68%, open circuit voltage of 0.96V, and short circuit current of 34.8 mA/cm^{-2} at 1 μm thickness. Analyzing the data, we observed that changing thickness between this range effect on parameters is very low.
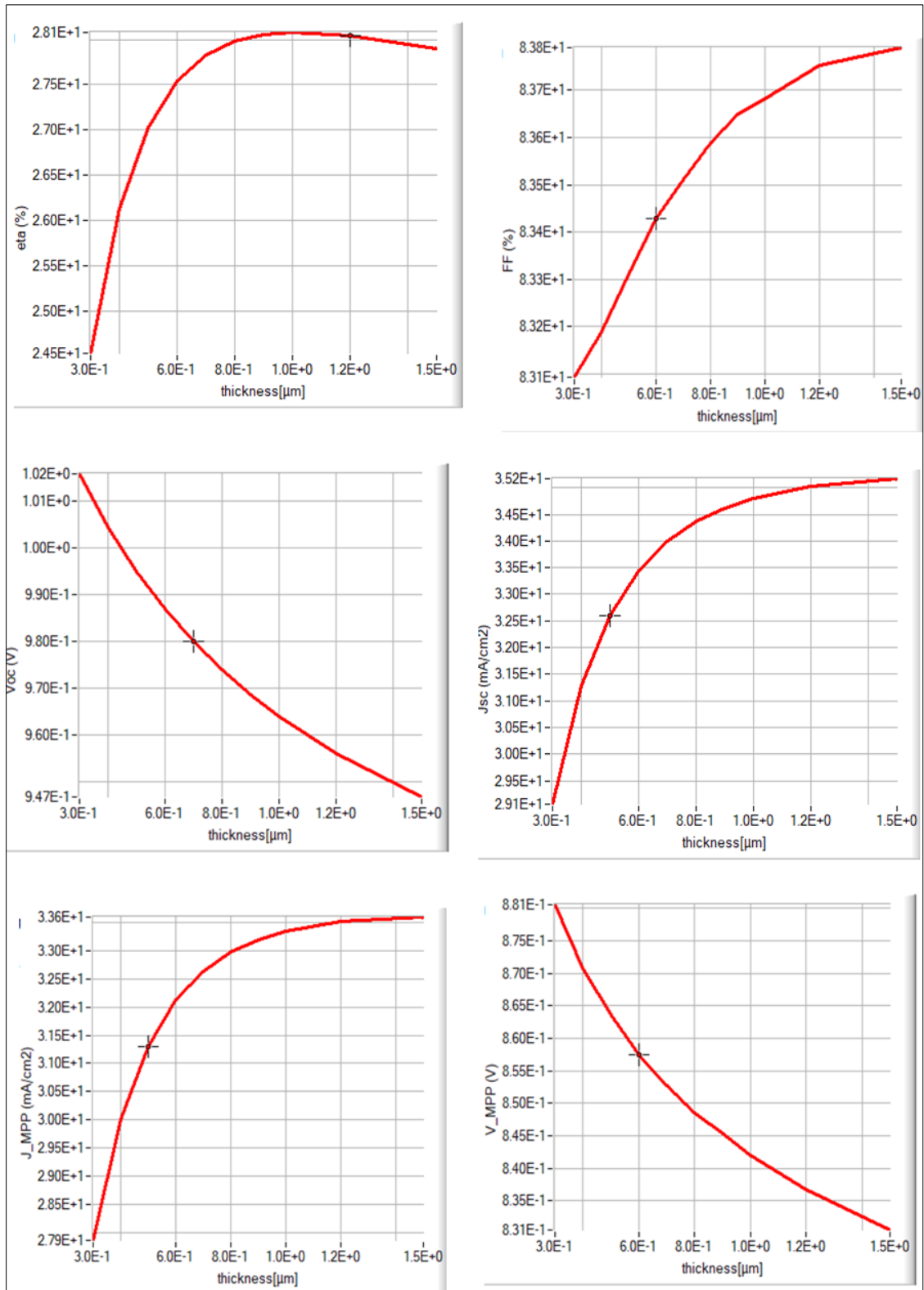
Figure 3 Effect of thickness on Electrical properties of Solar cell

According to the results, as the thickness increases, the Fill Factor (FF) is sparely changed. Other performance parameters Voc and V_mpp decline with an increase in thickness, and Jsc and J_mpp increase observed from the curve. Figure 4, shows current density vs efficiency and wavelength vs quantum efficiency. The effect of thickness on the J-V curve performance changes with an increase in thickness. 100% quantum efficiency is showing approximately 370 nm to 600 nm wavelength in 0.7 µm thickness. QE varies quickly after varying thickness.
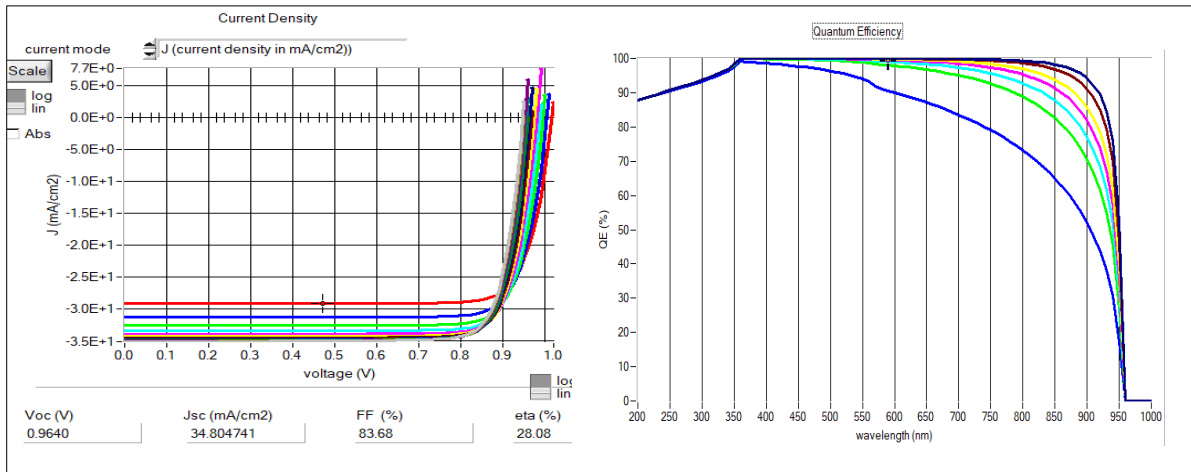
Figure 4 Effect of thickness on I-V curve and quantum efficiency(QE)

3.3. Effect of Bandgap on Electrical Properties of Solar Cells
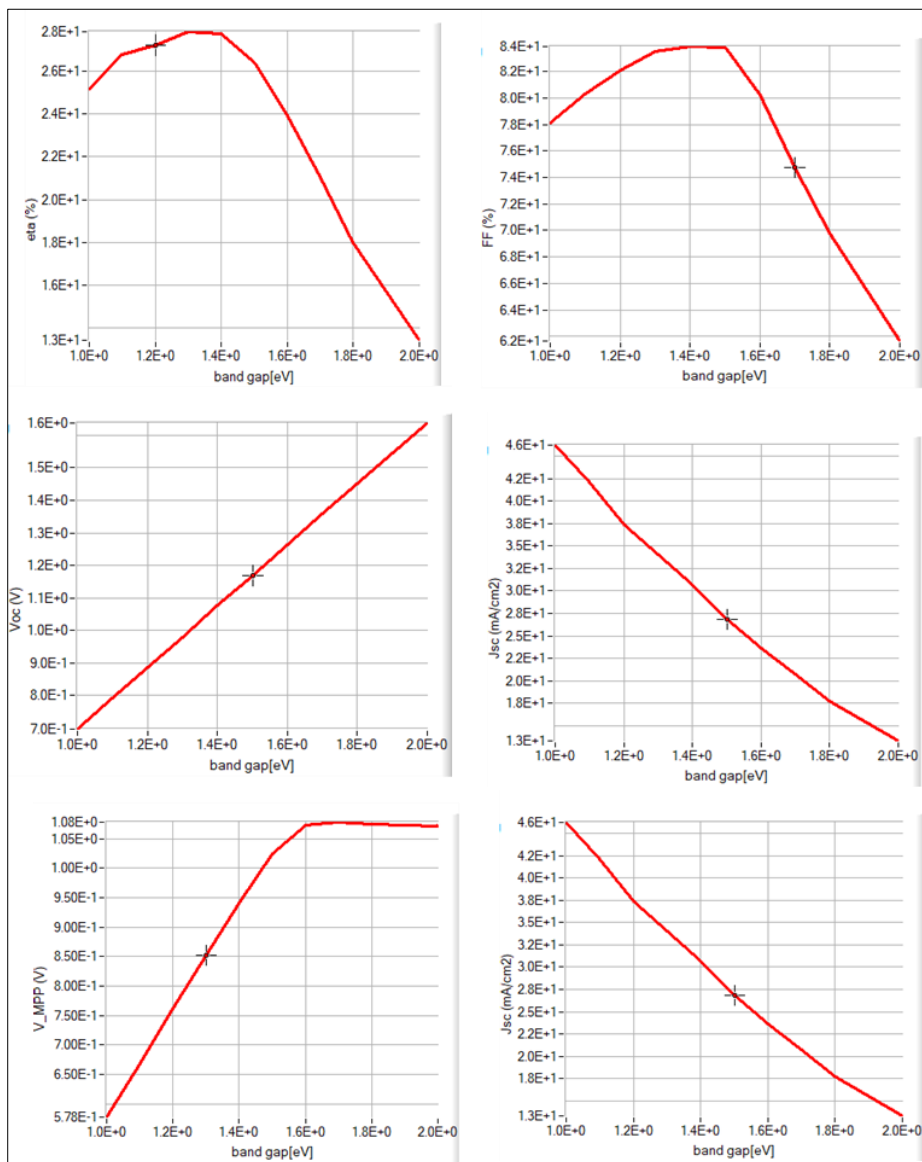
Figure 5 Demonstrates the relation between bandgap and device performance

The results represent a clear relation between bandgap energy and device performance shown in Figure 5. In this portion, the band gap varies between 0.3eV to 2eV, Efficiency increases with the increase of bandgap initially (0.3eV to 1.3eV), and later efficiency declines faster. Here the 1.3eV bandgap gives the optimum reading. The fill factor decreases after 1.5eV and the maximum fill factor we get is 84% in 1.4eV. Voc increases with band gap as a ramp function, V_mpp exponentially increases at a point 1.6eV, and Jsc, J-mpp decreases with increased bandgap. Maximum efficiency has been reported in 1.3eV and the maximum fill factor has been reported in 1.4eV. Regarding the better performance, it is clear that the bandgap of 1.3eV with a PCE of 28% can be the optimum choice for the $CH_3NH_3Sn(I_{1-x}Cl_x)_3$ layer. Demonstrate the changes in the doping band gap affect the performance of the semiconductor device $CH_3NH_3Sn(I_{1-x}Cl_x)_3$ absorber layer.

3.4. Effect of absorber layer doping density

The doping density is an essential property of solar cells' various layers that change in doping density to affect the solar cell's performance. Here, the absorber acceptor density NA has been studied in the 1×10^2 cm^{-3} to 2×10^{21} cm^{-3}, with the optimized thickness and bandgap, and the performance graph was obtained. At the same time, donor density ND (1/cm3) has taken zero. Figures 6 represent PCE and other electrical properties as a function of the acceptor doping density of the absorber layer. PCE gets a maximum of 35.65% at 1×10^{20} 1/cm^3 which is the best performance of the device.
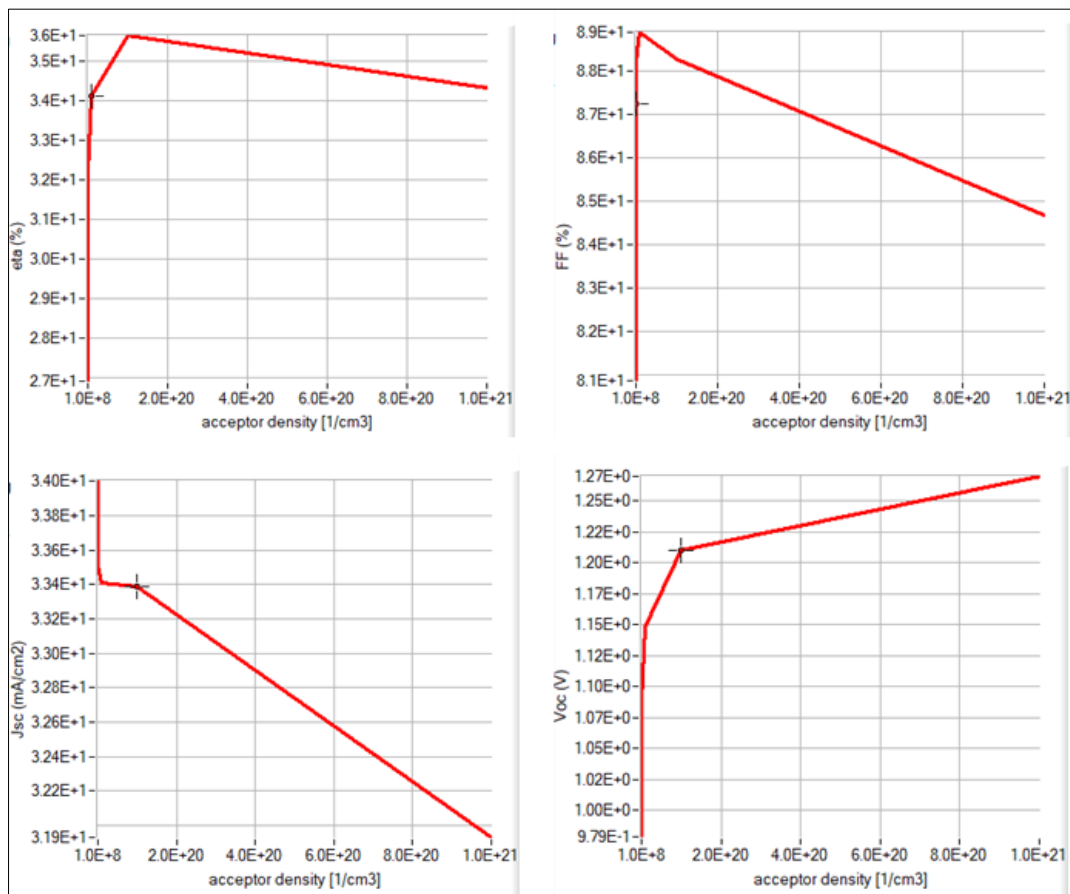
Figure 6 Effect of absorber layer doping density on electrical performance

At optimized doping concentration, the FF of 88.26, Voc 1.21V, and Jsc of 33.38mA/cm^{-2}, is obtained. From Figure 6 we noticed that the FF, Voc, V_mpp is increased and Jsc, J_mpp decreases according to the increase in the absorber layer acceptor doping density.
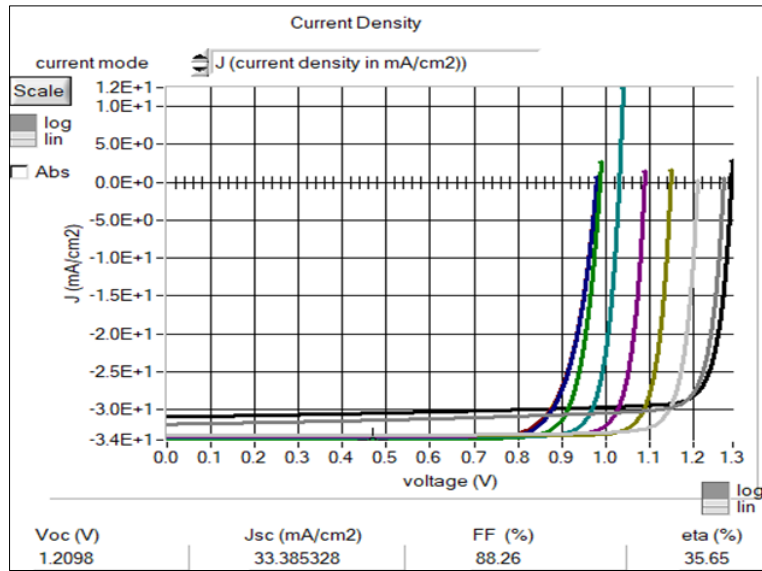
Figure 7 I-V curve for Effect of acceptor density NA

3.5. Effect of defect density

In this study, the defect density has been varied from 10^{10} cm^{-3} to 10^{18} cm^{-3} and picturized its variation on photovoltaic properties in PSC, as shown in Figure 8.
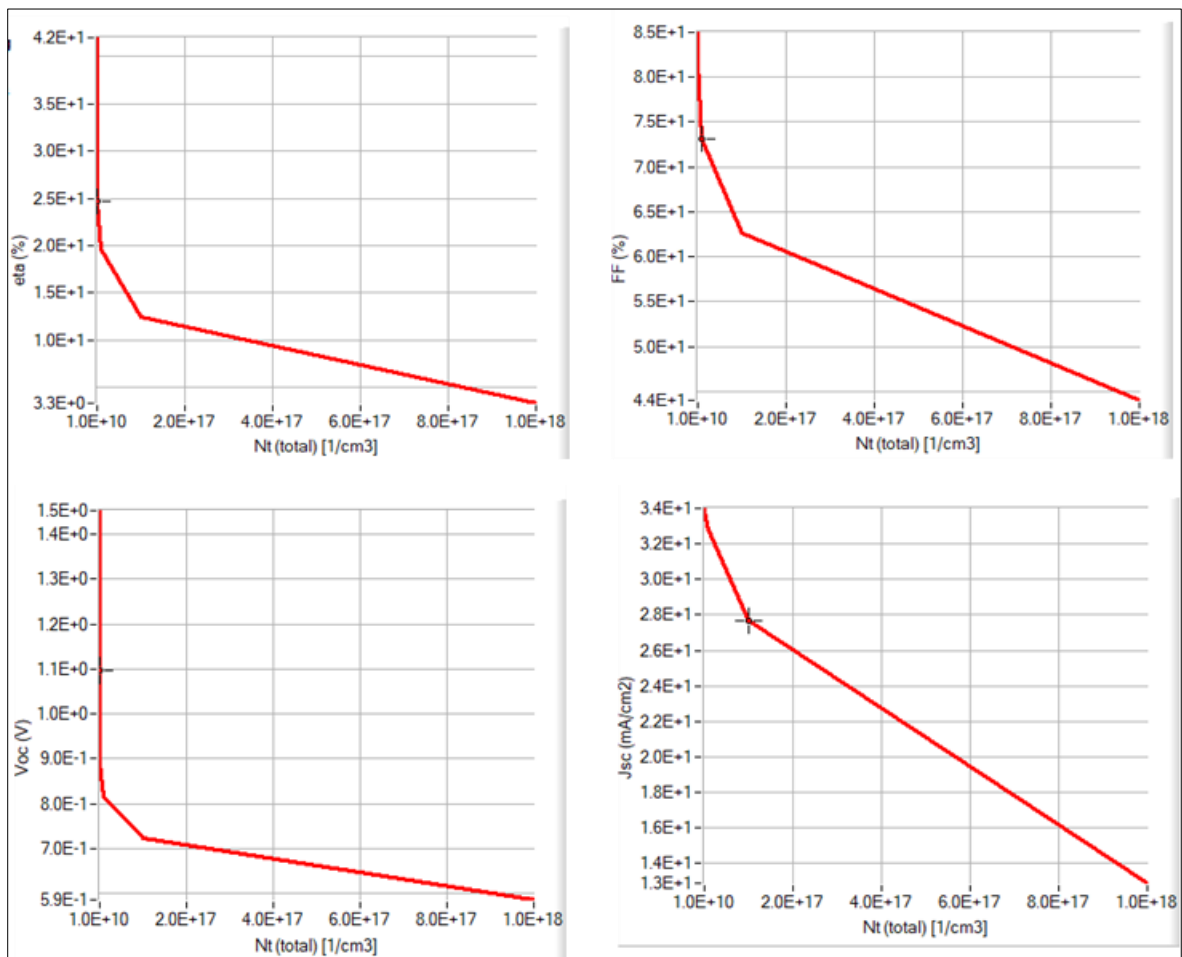
Figure 8 Solar cell response as a function of defect density

It is noticed that the performance of the device declined from 27.83% to 3.32% with the increase in defect density. The absorber layer's initial defect density was set to be 1×10^{14} cm^{-3} (as per Table 1) [17]. When the defect density is 10^{13} per cm^{-3}, the cell performance is significantly improved, attaining the Voc of 1.1 V, Jsc of 34.01 mA/cm2, FF of 82.14%, and PCE of 30.62%. Now, further decrease of total detect density-Nt, from 1×10^{13} to 1×10^{12} cm^{-3}, minor variation is observed in FF (82.94.78%) and Jsc (34.02mA/cm^2) but considerable changes occurred in Voc (1.21 V) and PCE (34.27%).

3.6. Optimized result and I–V curve

We have observed the effect of thickness, bandgap, acceptor density, and defect density on the absorber layer, and the optimum value obtained from the resulting value in Table 2.

Table 2 Optimal and selected values for absorber layer

Type	Thickness (μm)	Band Gap (eV)	Acceptor density NA (1/cm3)	Total Defect density, Nt (1/cm3)
Previous value	0.7	1.3	3.2×10^{15}	1×10^{14}
Optimum value	0.9	1.3	1×10^{20}	1×10^{13}

After setting the optimum data as device parameters and simulating data to achieve the performance of the solar cell which is shown much better efficiency than the selected value, the final J-V curve was obtained and represented in Figure 9.
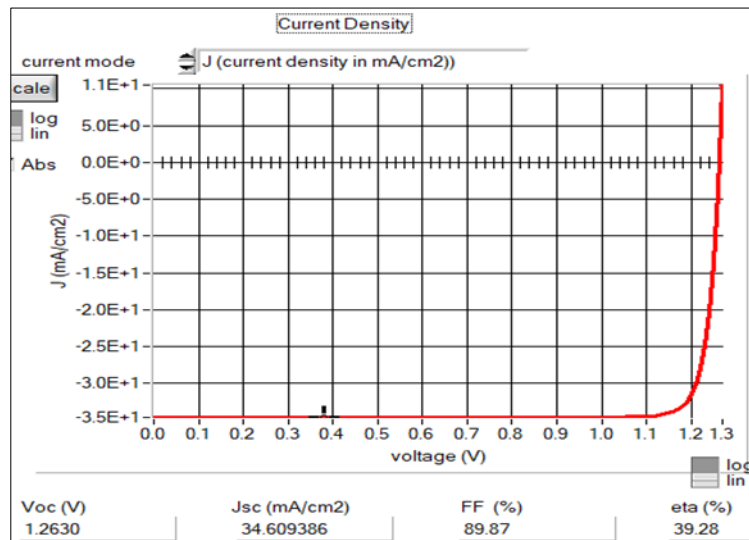
Figure 9 J-V curve of the perovskite solar cell at optimum values

Table 3 Comparative analysis of Figure 2 and 9 diagrams

Step1	Voc (V)	Jsc (mA/cm^2)	FF%	PCE%
Primary value	0.98	33.39	83.51	27.83
Optimum value	1.26	34.61	89.87	39.28

It is noticed that the efficiency of the solar cell has jumped from 27.83% to 39.28%.

4. Conclusion

In this study, a numerical simulation of a planar heterojunction tin-based $CH_3NH_3Sn(I_{1-x}Cl_x)_3$ PSCs has been performed using SCAPS-1D. It has been observed that the PSCs efficiency may improve by selecting the optimum value thickness and doping acceptor density NA absorber layer. The optimum value of thickness is .09µm and the optimized doping concentration is 10^{20} cm^{-3}. We achieved an efficiency of 39.28%, Voc of 1.26V, FF of 89.87%, and Jsc of 34.61 mA/cm^2. The effect of defect density and doping concentration plays a major role in improving the Fill factor and efficiency.

References

[1]   https://doi.org/10.1021/acs.biochem.8b00603

[2]   Kojima, Akihiro; Teshima, Kenjiro; Shirai, Yasuo; Miyasaka, Tsutomu (May 6, 2009). "Organometal Halide Perovskites as Visible-Light Sensitizers for Photovoltaic Cells". Journal of the American Chemical Society. 131 (17): 6050–6051. doi:10.1021/ja809598r. PMID 19366264

[3]   Best Research-Cell Efficiencies (PDF). National Renewable Energy Laboratory. 2022-06-30. Archived from the original (PDF) on 2022-08-03. Retrieved 2022-07-12

[4]   Helmholtz-Zentrum Berlin für Materialien und Energie. "World record again at HZB: Almost 30 % efficiency for next-generation tandem solar cells". HZB Website.

[5]   DOI: https://doi.org/10.1038/s41598-023-44845-6

[6]   DOI: http://dx.doi.org/10.15377/2410-2199.2021.08.3

[7]   Nalianya, M. A. et al. Numerical study of lead-free CsSn0.5Ge0.5I3 perovskite solar cell by SCAPS-1D. Optik 248, 168060 (2021).

[8]   Abdelaziz, S., Zekry, A., Shaker, A. & Abouelatta, M. Investigation of lead-free MASnI3-MASnIBr2 tandem solar cell: Numerical simulation. Opt. Mater. 123, 111893 (2022).

[9]   Kanoun, A.-A., Kanoun, M. B., Merad, A. E. & Goumri-Said, S. Toward development of high-performance perovskite solar cells based on CH3NH3GeI3 using computational approach. Sol. Energy 182, 237–244 (2019).

[10]   Ahmmed, S. et al. CuO based solar cell with V2O5 BSF layer: Teoretical validation of experimental data. Superlattices Microstruct. 151, 106830 (2021)

[11]   Lazemi, M., Asgharizadeh, S. & Bellucci, S. A computational approach to interface engineering of lead-free CH3NH3SnI3highly-efcient perovskite solar cells. Phys. Chem. Chem. Phys. 00, 1–10 (2018)

[12]   Ma, L. et al. Carrier difusion lengths of over 500 nm in lead-free perovskite CH3NH3SnI3 flms. J. Am. Chem. Soc. 138, 14750–14755 (2016).

[13]   Lin, L., Jiang, L., Li, P., Fan, B. & Qiu, Y. A modelled perovskite solar cell structure with a Cu2O hole- transporting layer enabling over 20% efciency by low-cost low-temperature processing. J. Phys. Chem Solids 14, 205–211 (2019).

[14]   Yang, H. Y., Rho, W. Y., Lee, S. K., Kim, S. H. & Hahn, Y. B. TiO2 nanoparticles/nanotubes for efcient light harvesting in perovskite solar cells. Nanomaterials 9, 326–335 (2019).

[15]   Yu, W. et al. Ultrathin Cu2O as an efcient inorganic hole transporting material for perovskite solar cells. Nanoscale 00, 1–3 (2015).

[16]   Yu, S., Li, L., Lyu, X. & Zhang, W. Preparation and investigation of nano-thick FTO/Ag/FTO multilayer transparent electrodes with high fgure of merit. Sci. Rep. 6, 20399–20406 (2016).

[17]   S. Heo et.al., Deep level trapped defect analysis in CH3NH3PbI3 perovskite solar cells by deep level transient spectroscopy, Energy Environ Sci. 10 (2017) 1128, doi: 10.1039/c7ee00303j.